Supporting Information

Nanozymes with versatile redox capabilities inspired in metalloenzymes

Rocío López-Domene[a,b], Krishan Kumar[a], Jose Eduardo Barcelon[c], Gabriela Guedes [b], Ana Beloqui[a,d], Aitziber L. Cortajarena[b,d]**

[a] POLYMAT and Department of Applied Chemistry, Faculty of Chemistry, University of the Basque Country UPV/EHU.
Paseo Manuel Lardizabal 3, Donostia-San Sebastián, 20018, Spain

[b] Center for Cooperative Research in Biomaterials (CIC biomaGUNE), Basque Research and Technology Alliance (BRTA)
Paseo de Miramón 194, Donostia-San Sebastián, 20014, Spain

[c] Donostia International Physics Center
Paseo Manuel de Lardizabal 4, 20018 Donostia-San Sebastian, Spain

[d] IKERBASQUE, Basque Foundation for Science
Plaza Euskadi 5, Bilbao, 48009, Spain

INDEX

1. Materials

Chloroauric acid ($HAuCl_4$), potassium tetrachloroplatinate (K_2PtCl_4), sodium ascorbate (SA), 1,2,3-trihydroxybenzene, also named pyrogallol (PG), 2,2-Azino-bis(3-ethylbenzothiazoline-6-sulfonic acid) diammonium salt (ABTS), 3,3′,5,5′-Tetramethylbenzidine (TMB), and sodium phosphate monobasic (NaH_2PO_4), p-nitrophenol, p-nitrophenyl butyrate (PNB), *Candida Antarctica* Lipase B (CALB) and other chemicals were purchased from Sigma Aldrich and used without further purification. Fresh working solutions were prepared by diluting the stock solutions with water and adjusting the pH, if necessary, using either HCl or NaOH. The concentration and purification of CTPR protein and NCs@CTPR hybrids were accomplished using filter membranes (Amicon®Ultra 0.5 mL and 15 mL, 10 kDa MWCO) and dialysis membranes (SnakeSkin, ThermoFisher, 10 kDa MWCO).

2. Instrumentation

2.1. Ultraviolet–visible spectroscopy (UV-Vis)

UV-visible measurements were conducted using a Synergy H1 Hybrid Multi-Mode Microplate Reader that was controlled by Gen5 Software. The spectral data were collected within the wavelength range of 250 nm to 800 nm, using a step size of 2 nm. To eliminate the contribution of the buffer, the absorbance spectrum of the buffer was subtracted from all the measured spectra.

2.2. Transmission Electron Microscopy (TEM) Imaging

TEM samples were prepared by drop-casting of each sample onto ultrathin Lacey carbon films on copper grids, 200 mesh (TED PELLA INC.). Initially, the grids were treated by plasma discharge for 10 min. Afterwards, the samples were deposited by drop-casting of 0.5 μL of each protein-nanocluster sample dispersed in water at a protein concentration of around 10 μM. Micrographs were captured using a JEOL JEM 1400 Plus microscope (80 kV). The nanoparticle sizes were determined by measuring 100 particles using ImageJ software.

2.3. Matrix-Assisted laser desorption ionization mass spectrometry (MALDI-ToF)

Matrix-Assisted Laser Desorption/Ionization time-of-flight (MALDI-ToF) spectra were acquired using a MALDI/ToF-ToF MS UltrafleXtreme III (Bruker) mass spectrometer equipped with a delayed extraction and a pulsed N_2 laser (λ = 337 nm) controlled by Flex Control 3.3 software. The thin layer method was employed for the MALDI-ToF sample preparation.[1] To prepare a thin layer, a drop of saturated solution of α-Cyano-4-hydroxycinnamic acid (α-CHCA) in acetone was deposited on the MALDI target. The matrix

solution was prepared by mixing a 1:1 ratio (v/v) of 10 mg mL^{-1} of α-CHCA in acetonitrile (ACN) and 5% formic acid (70:30, v/v) and 10 mg mL^{-1} of DHB (2,5- dihydroxybenzoic acid) in ACN and 0.1% TFA (trifluoroacetic acid) (70:30, v/v). Finally, 1 µL of the sample was mixed with 2 µL of the matrix solution and deposited onto the MALDI plate, after which it was allowed to air-dry before analysis.

2.4. Inductively coupled plasma mass spectrometry (ICP-MS)

To determine the amount of Au and Pt, 150 µL of 29, 41, 44, 73, and 172 µM of Pt_{11}, Pt_{16}, Pt_{34}, Pt_{46}, and Au_7Pt_{74}, respectively were mixed with 2850 µL of aqua regia, and the resulting suspension was sonicated at 40ºC for 30 minutes. Subsequently, 2 mL of distilled water was added to the mixture. The sample was analyzed using an iCAP-Q ICP-MS (Thermo Scientific, Bremen, Germany) equipped with an autosampler A-520 (Cetac Technologies Inc., NE, USA) (n = 3) and QtegraTM v2.6 (Thermo Scientific).

2.5. X-ray photoelectron spectroscopy (XPS)

X-ray photoelectron measurements were conducted using a Phoibos-100 electron analyzer (SPECS GmbH) with a non-monochromatic Al Ka photon source at 1486.6 eV. All the spectra were calibrated to the sp3 (C-C) component of the C1s spectrum centered at 284.8 eV. Fits were performed in KolXPD software. The samples were deposited on silicon oxide wafers. All the measurements were performed under ultra-high vacuum (UHV) conditions (XPS vacuum chamber is kept at a pressure of 1×10^{-9} mbar or lower).

3. Design, expression, purification, and characterization of CTPR proteins

3.1. Design of CTPR modules.

An engineered consensus tetratricopeptide repeats (CTPR) protein with six repeats and a histidine-binding module ($C6_{His}$ protein) was created as reported before.[2] The coordinating residues were inserted at positions 2, 5, 6, and 9 of the CTPR motif. To enhance the solubility of the protein the engineered CTPRs included an additional C-terminal solvating helix with polar residues.

3.2. Expression and purification of CTPR protein.

Protein was produced using a synthetic gene encoding the $C6_{His}$ protein inserted into the ampicillin-resistant pProEx-HTA vector, which encoded an N-terminal hexa-histidine tag. Expression of the protein was performed in *Escherichia coli* C41 (DE3) upon induction with 1 mM isopropyl β-d-thiogalactoside (IPTG) at an optical density between 0.6 and 0.8. The

induced cells were then grown, at 20 °C for 18 hours. To extract the proteins, the cell pellets were suspended in a lysis buffer containing 500 mM sodium chloride, 500 mM urea, and 50 mM Tris-HCl at pH 8.0. Sonication was employed to lyse the cells, after which the resulting pellet was frozen at -20 °C for at least one day. The protein was subsequently purified from the supernatant using a standard Ni-NTA affinity purification protocol. To remove the N-terminal hexa-histidine tag from the CTPR protein, the Tobacco Etch Virus (TEV) protease was employed. TEV protease was also expressed and purified using established protocols. Finally, the CTPR protein was dialyzed with 150 mM sodium chloride, and 50 mM phosphate buffer at pH 7.4, at a temperature of 4 °C, using a dialysis membrane with a molecular weight cutoff ranging from 6 to 8 kDa. Protein concentration was determined using UV-VIS spectroscopy at 280 nm, with the molar extinction coefficients derived from the amino acid composition. (ε=74720 M^{-1} cm^{-1}).

4. Synthesis and purification of the nanozymes

4.1. Synthesis and purification of the nanozymes.

For the synthesis of protein-templated metal nanoclusters (NCs), a modified synthesis method was employed.[3] The protein sample, initially in phosphate-buffered saline (PBS) containing 50 mM of PB and 150 mM of NaCl at pH 7.0, was adjusted to pH 10 using PD 10 desalting column. Subsequently, $C6_{His}$ protein (1 mL at 20 μM in PBS at pH 10) was incubated with the respective metal salts, allowing coordination with the histidine residues. This mixture underwent a 30-minute incubation at 50 °C to facilitate the reduction of protein disulfide bonds. The specific equivalents of metal salts used are documented in **Table S1** and include chloroauric acid ($HAuCl_4$), and potassium tetrachloroplatinate (K_2PtCl_4). Following the initial incubation, the reduction of metal salts was achieved using sodium L-ascorbate (SA) at 0 ºC for 10 minutes. The reaction mixtures were heated to 50 °C and stirred at 800 rpm for 72 hours. Sodium L-ascorbate was added in a molar excess of 100 relative to the metal concentration in each reaction. To remove the undesired large insoluble aggregates that formed, the samples were centrifuged at 4 °C and 15000 rpm for 1 hour. The supernatant obtained after centrifugation was collected and concentrated to 500 μL using Amicon filters with a cut-off of 10 kDa. The concentrated samples were then purified using a PD 10 desalting column. Protein concentration in the metal nanoclusters was estimated using BCA assay, employing dilutions of Pt-based nanozymes.

5. Compositional characterization of the protein-templated nanozymes

5.1. Yields

The protein concentration before and after the synthesis was quantified using the BCA-protein concentration assay for the set of Pt-containing nanozymes. The synthesis yields varied from 72 to 90 %, showing that the protein was almost fully recovered after the different purification steps. In addition, it demonstrates the robustness of the CTPR scaffold when heated up to 50 ºC for 3 days at pH 10 because no significant loss of protein was observed.

Table S1. Synthesis recovery yields were obtained for the array of samples built in this work.

No. Reaction	***Offered metal concentration (mM)***	***Offered Pt equivalents***	***Offered Au equivalents***	***Final composition***	***Synthesis Yield (%)***
1	0.6	32	-	Pt_{11}	72
2	1.28	64	-	Pt_{16}	80
3	3.2	160	-	Pt_{34}	80
4	6.4	320	-	Pt_{46}	89
5	1.28	320	32	Au_7Pt_{74}	90

5.2. TEM

The size of the synthesized NC was determined by TEM for all the samples, expect for Pt_{11}, which did not display measurable nanomaterials on the TEM micrographs.

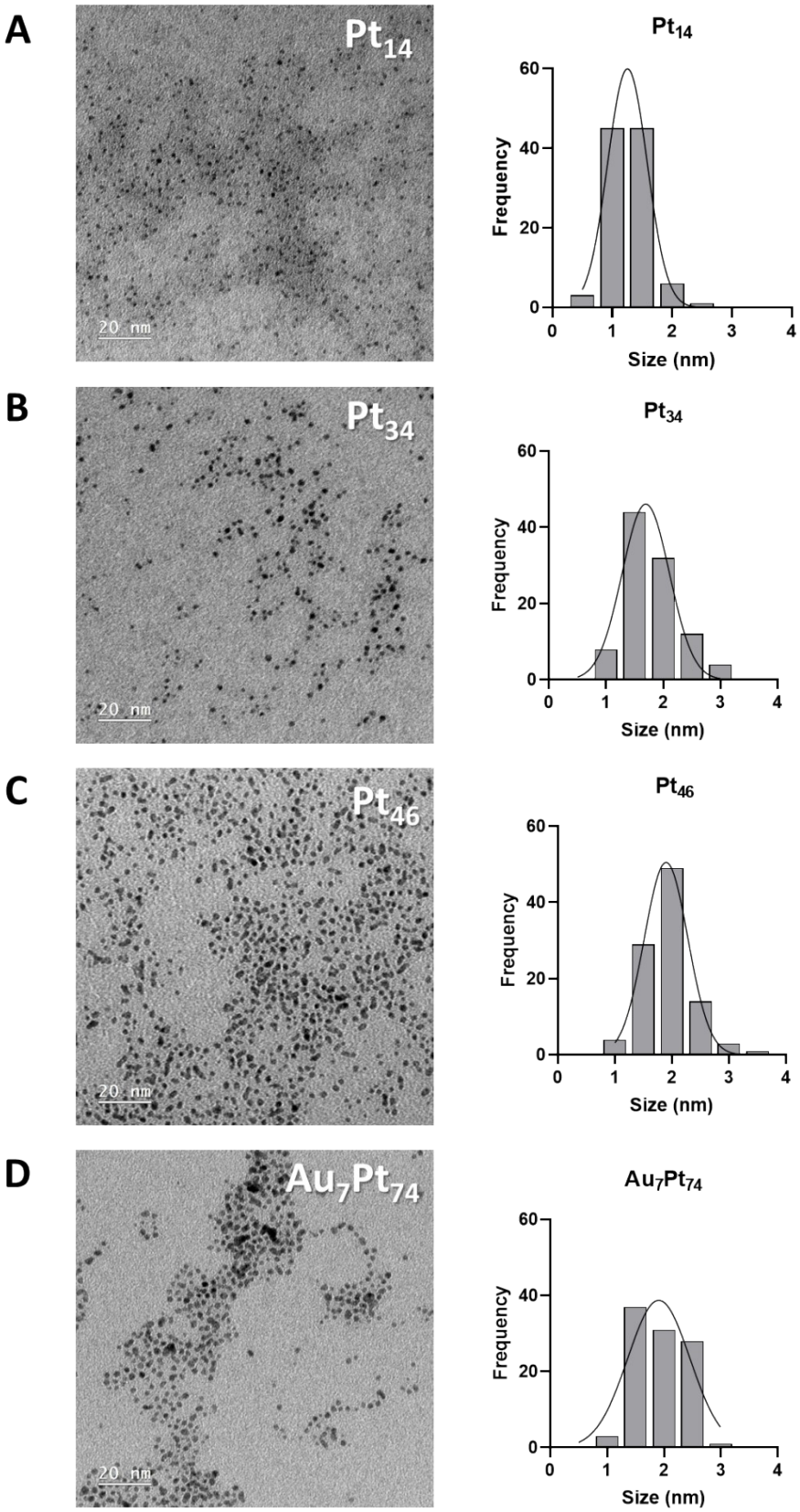

Figure S1. TEM images and size histogram for A) Pt_{14}, B) Pt_{34}, C) Pt_{46}, and D) Au_7Pt_{74}. *For Pt_{11}, no mNCs were observed.

Table S2. Size in nm of the different of mNCs calculated with ImageJ software of 100 mNCs in each TEM image.

Sample	Size (nm)
Pt_{14}	1.29 ± 0.32
Pt_{34}	1.81 ± 0.43
Pt_{46}	1.94 ± 0.42
Au_7Pt_{74}	1.95 ± 0.42

5.3. MALDI-ToF

The molecular weight of the different Pt-based nanozymes was analyzed by MALDI-ToF spectrometry and compared to the free protein. The experimental mass obtained for the $C6_{His}$ proteins was 26200 g mol^{-1}. Note that only the free protein and the hybrids with low Pt content (Pt_{11}, Pt_{16}, and Pt_{34}) could be detected by MALDI-ToF. The larger the nanocluster, the lower the S/N ratio was achieved. This decrease in the sensitivity could be attributed to the poor quality of the matrix crystals in the presence of the larger nanoclusters, resulting in low energy transfer from the matrix, and consequently limited efficiency to make the analyte sublimate and eventually fly through the ToF detector. The results collected in **Figure 1B** evidence that (1) there is no free protein, easily detected by MALDI-ToF, in the mixture and (2) there is an evident increase of m/z for the detected nanozymes (**Figure 1B**). As the analysis of the hybrids using MALDI-ToF is qualitative, the quantification of the metal content, which provides accurate information about the size of the nanocluster, is performed by ICP-MS.

5.4. ICP-MS

The sample preparation was performed by the addition of 150 µL of the nanozyme solution to 500 µL of a solution of aqua regia. The digestion of the samples was carried out overnight. Thereafter, 2.85 mL of deionized water were added. The samples were analyzed using an iCAP-Q ICPMS and Pt concentration calculated according to calibration standards.

Table S3. Collected results from ICP-MS measurements.

Nº Reaction	**[protein] /µM**	**[metal] / µM**	**Pt/Au atoms per protein**	**Code**
1	41	450 ± 78	10.9 ± 0.85	Pt_{11}
2	29	447 ± 35	15.9 ± 2.70	Pt_{16}
3	44	1487 ± 54	33.8 ± 1.24	Pt_{34}
4	73	3368 ± 46	46.1 ± 0.64	Pt_{46}
5	172	Pt: 12682 ± 275 Au: 1255 ± 10	73.7 ± 1.6 7.30 ± 0.06	Au_7Pt_{74}

5.5. XPS

The XPS spectra of the nanozymes were measured, and the Pt4f and Au4f components were analyzed. Samples were directly mounted on a flag-type sample holder with copper tape. All the samples were measured in UHV with photon energy set to 1486.6 eV (Al Kα). The fits shown in Figure S1 and S2 are the core level spectra modeled as a Voigt function (doublet) convoluted with a Shirley type background.

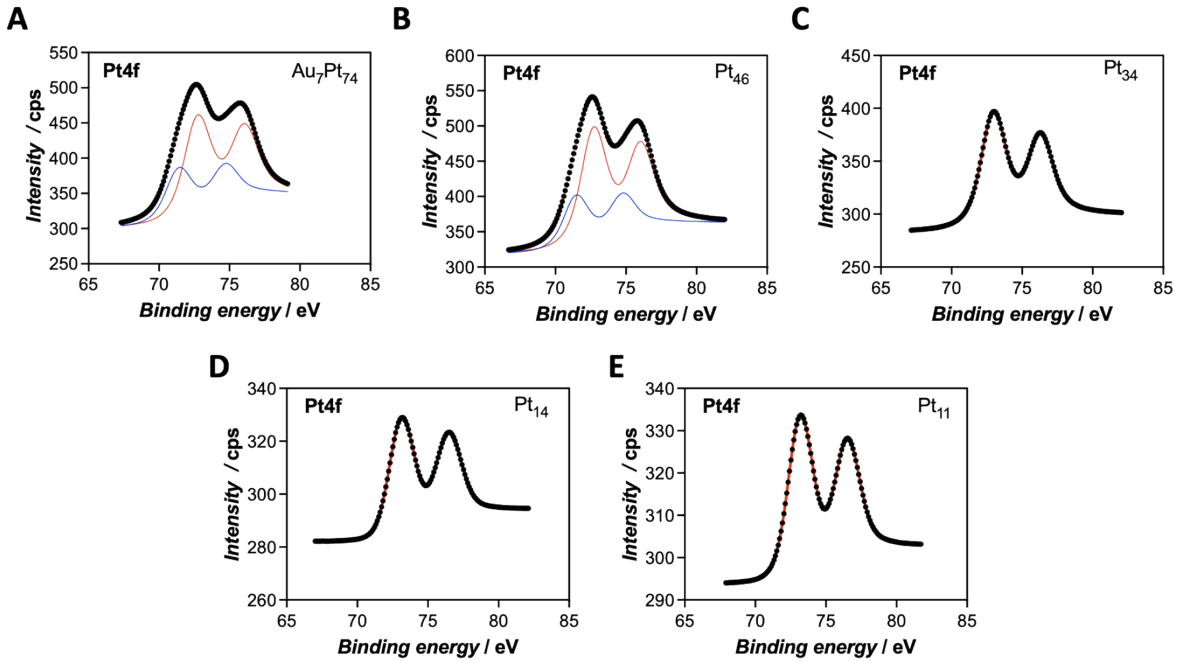

Figure S2. XPS spectra of the Pt4f component for each of the nanozymes: A) Au_7Pt_{74}; B) Pt_{46}; C) Pt_{34}; D) Pt_{14}; and E) Pt_{11}. A) and B) spectra could be deconvoluted into 2 Pt species which presumably correspond to Pt^{II} and Pt^0.

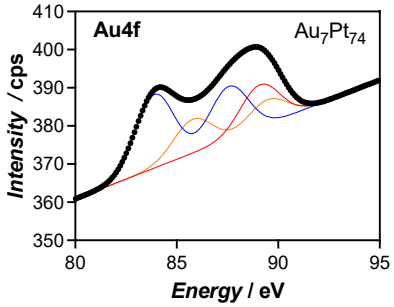

Figure S3. Au4f spectrum measured for the Au_7Pt_{74} nanozyme. The spectrum shows a contribution of the silicon wafer used for the measurements (red component).

6. Redox catalytic performance of the nanozymes

6.1. Oxidation capability

6.1.1. Oxygen consumption

The consumption of oxygen along the oxidation reactions was measured with a PICO-O2 fiber-optical oxygen meter connected to the oxygen dipping probe OPDIP20 from PyroScience GmbH. These measurements were carried out with all the set of nanozymes. For these measurements, the substrate, pyrogallol, was added at 3 mM in a PBS solution that was kept at 25 ºC. A stabilization period of 60 seconds was applied to achieve a stable measurement of oxygen concentration. Thereon, 20 µL of nanozyme were added at different protein concentrations from (1-10 µM) and the oxidation reaction was carried out until the oxygen present in the solution was consumed. Four experiments were performed with N=3 technical replicates forAu_7Pt_{74}.

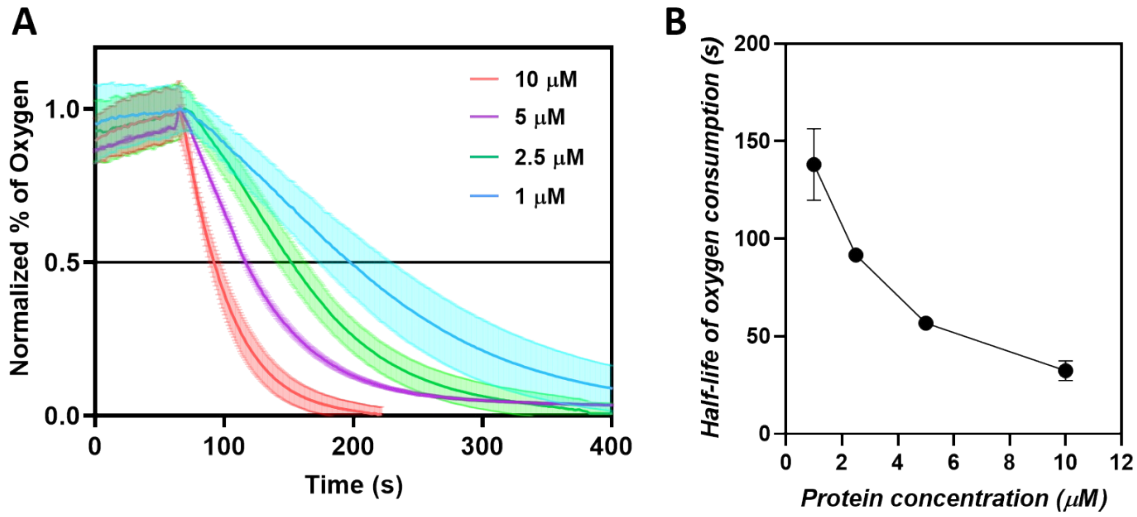

Figure S4. A) Oxygen consumption measured with a PICO-O2 fiber-optical oxygen meter at 1-10 µM of protein concentration of Au_7Pt_{74}. B) Representation of the time needed to consume the 50% of the oxygen in the medium for each of the concentrations measured.

To compare the oxidation efficiency between the different nanozymes, we calculated the OC50, defined as the time needed to consume the 50% of the oxygen present in the medium. The faster the oxidation, the lower OC50 was shown in Table S3.

Table S4. OC50 measured for all the nanozymes under same reaction conditions (3 mM of PG, 5 µM of nanozyme in PBS at 25ºC)

Sample	OC50 / s

Au_7Pt_{74}	50 ± 1
Pt_{46}	83 ± 3
Pt_{34}	293 ± 2
Pt_{16}	770 ± 22
Pt_{11}	> 1400

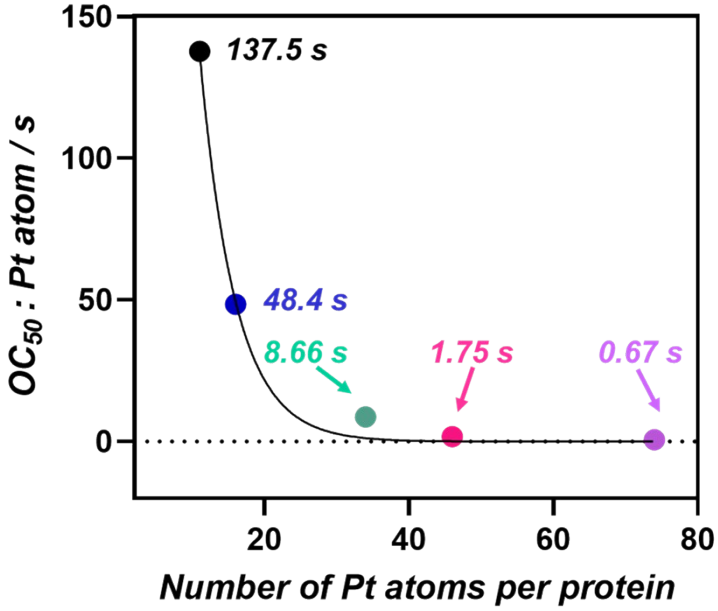

Figure S5. Representation of the oxygen consumption rate (as OC50) normalized per Pt atoms for each nanocluster: Pt11 (in black), Pt16 (blue), Pt34 (green), Pt46 (pink), and Au7Pt74 (purple). This representation reveals an exponential correlation between the number of Pt atoms and the activity showed by the hybrids, with higher activity corresponding to lower OC50 values. This exponential correlation was fitted using GraphPad software to an exponential growth equation (black line), resulting in the following equation: $y = 1310 * \exp^{(-0.20 * x)}$. The goodness of fit was $R^2 = 0.9956$.

6.1.2. Kinetic Measurements – oxidation

In this study, we investigated the oxidase potential of the synthesized array of nanozymes. We utilized three chromogenic substrates, namely pyrogallol (PG), 2,2'-azino-bis(3-ethylbenzothiazoline-6-sulfonic acid) (ABTS), and 3,3′,5,5′-Tetramethylbenzidine (TMB), to evaluate the oxidation capability of Pt_{11},Pt_{16},Pt_{34},Pt_{46},and Au_7Pt_{74}. The oxidation kinetics followed the Michaelis-Menten model, commonly employed to analyze the kinetic profiles of natural enzymes.

First, the oxidation of PG was assessed at same protein concentration (1 μM) for all the nanozymes set (**Figure S5**). In this experiment, we analyzed the catalytic potential of each hybrid, at a fixed PG concentration (3 mM) in 50 mM PB buffer at pH 7 and at 25 ºC. The reaction was tracked at 420 nm by UV-Vis measurements in real time. These results suggest that the Pt_{77} and Au_7Pt_{50} showed the highest reaction velocities, followed by the Pt_{20} hybrid. However, when analyzing Pt_7 and Pt_{14} at these reaction conditions almost no pyrogallol oxidation was exhibited. Initial velocities are used to plot the specific activity in **Figure 2B**.

Secondly, the oxidation of ABTS and TMB was monitored at 420 and 650 nm, respectively. The buffer used in this reaction was 50 mM sodium acetate at pH 5. Blanks were measured for each of the substrates. For each hybrid examined, experiments at different substrates concentrations (PG, TMB, and ABTS) and a fixed protein/catalyst concentration (1 μM) were carried out to calculate the apparent Michaelis-Menten constant ($^{app}K_M$) and the apparent maximum velocities ($^{app}V_{max}$) for the 3 active nanozymes. The apparent turnover number $^{app}k_{cat}$ for each hybrid and substrate was calculated at a fixed substrate concentration, 4 mM for PG and TMB, and 3 mM for ABTS, and at increasing catalyst concentrations. All the reactions were measured at its respective working buffer, pH 5 for ABTS and TMB, and pH 7 for PG at 25 ºC.

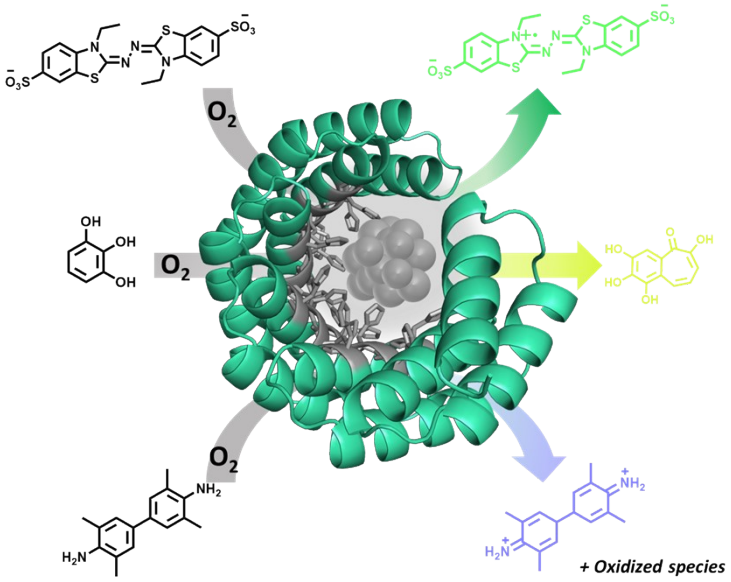

Figure S6. Oxidation reactions performed for the nanozyme set utilizing the non-chromogenic substrates (ABTS, PG, and TMB) and converting by the metal nanocluster to their respective oxidized products (Chromogenic products, ABTS in green, PG in yellow, and TMB in blue).

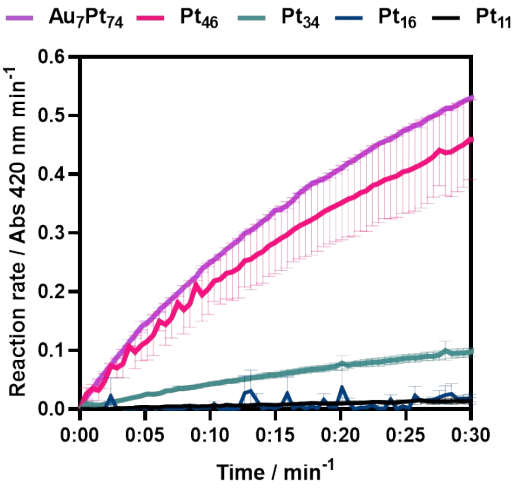

Figure S7. The reaction rate on the oxidation of PG is monitored at 420 nm. Pt_{16}, Pt_{11} did not show oxidation activity under these conditions.

Table S5. Kinetic parameters measured for the Au_7Pt_{74}, Pt_{46}, and Pt_{34}samples for the oxidation of ABTS.

Sample	$^{app}K_M$ (mM)	$^{app}V_{max}$ (μmol s^{-1} mg^{-1})	$^{app}k_{cat}$ (s^{-1})	$^{app}k_{cat}/K_M$ ($s^{-1}mM^{-1}$)
Au_7Pt_{74}	0.706 ± 0.157	0.214 ± 0.024	0.034 ± 0.005	0.061 ± 0.014
Pt_{46}	0.785 ± 0.299	0.230 ± 0.042	0.038 ± 0.006	0.048 ± 0.014
Pt_{34}	1.222 ± 0.570	0.047 ± 0.015	0.006 ± 0.001	0.005 ± 0.002

Table S6. Kinetic parameters measured for the Au_7Pt_{74}, Pt_{46}, and Pt_{34}samples for the oxidation of TMB.

Sample	$^{app}K_M$ (mM)	$^{app}V_{max}$ (μmol s^{-1} mg^{-1})	$^{app}k_{cat}$ (s^{-1})	$^{app}k_{cat}/K_M$ ($s^{-1}mM^{-1}$)
Au_7Pt_{74}	0.2155 ± 0.072	0.2812 ± 0.030	0.022 ± 0.003	0.102 ± 0.010
Pt_{46}	0.2188 ± 0.084	0.037 ± 0.005	0.021 ± 0.004	0.096 ± 0.012
Pt_{34}	0.176 ± 0.056	0.039 ± 0.004	0.003 ± 0.001	0.017 ± 0.002

Table S7. Kinetic parameters measured for the Au_7Pt_{74}, Pt_{46}, and Pt_{34} samples for the oxidation of PG.

Sample	$^{app}K_M$ (mM)	$^{app}V_{max}$ (μmol s^{-1} mg^{-1})	$^{app}k_{cat}$ (s^{-1})	$^{app}k_{cat}/K_M$ ($s^{-1}mM^{-1}$)
Au_7Pt_{74}	0.211 ± 0.039	2.883 ± 0.16	0.222 ± 0.045	1.052 ± 0.086
Pt_{46}	0.118 ± 0.034	2.136 ± 0.15	0.307 ± 0.061	2.602 ± 0.368
Pt_{34}	0.084 ± 0.038	0.4337 ± 0.050	0.101 ± 0.006	1.202 ± 0.147

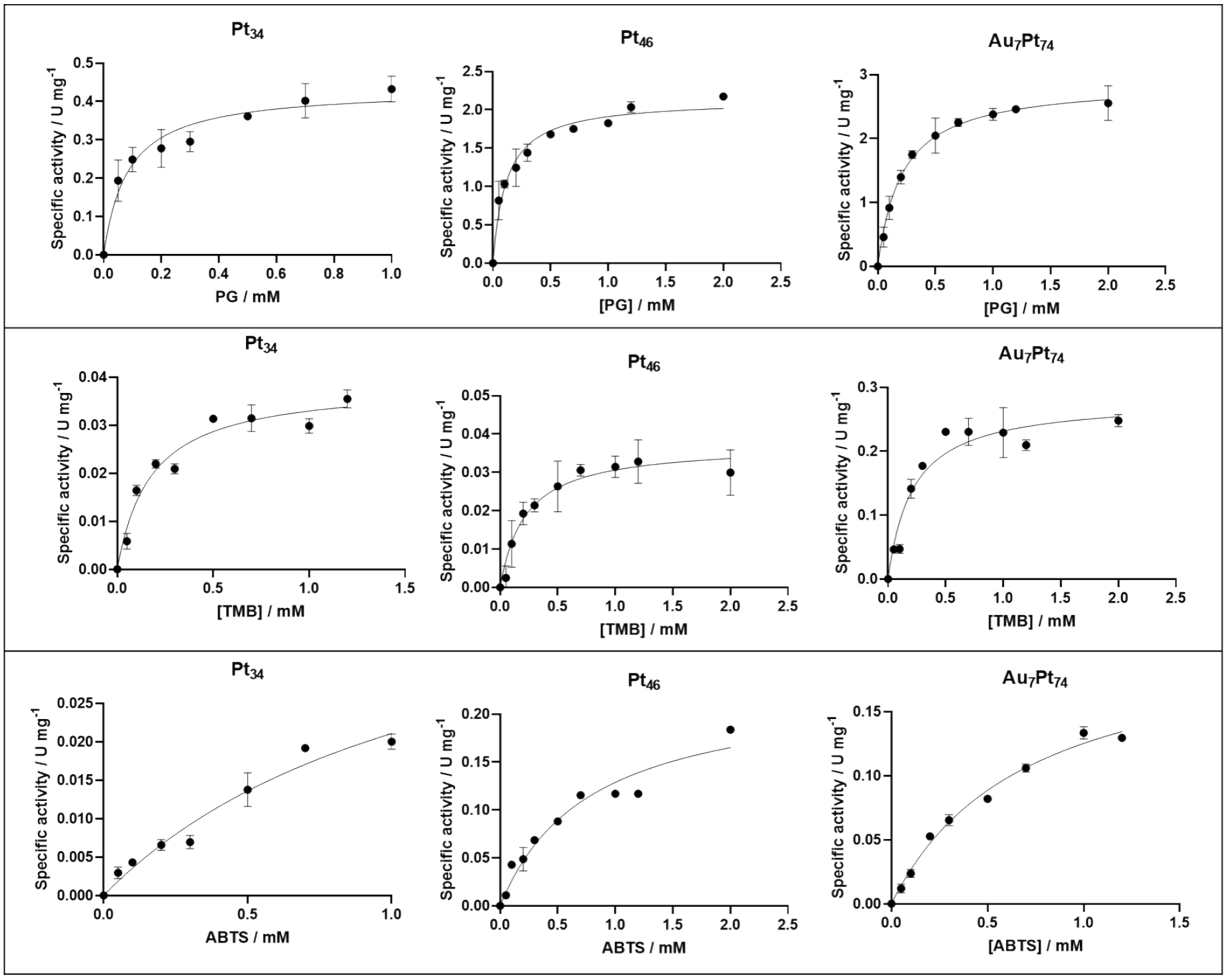

Figure S8. Michaelis-Menten profiles for A) PG, B) TMB, and C) ABTS for the nanozymes Pt_{34}, Pt_{46} and Au_7Pt_{74}, stabilized by the $C6_{His}$ CTPR protein.

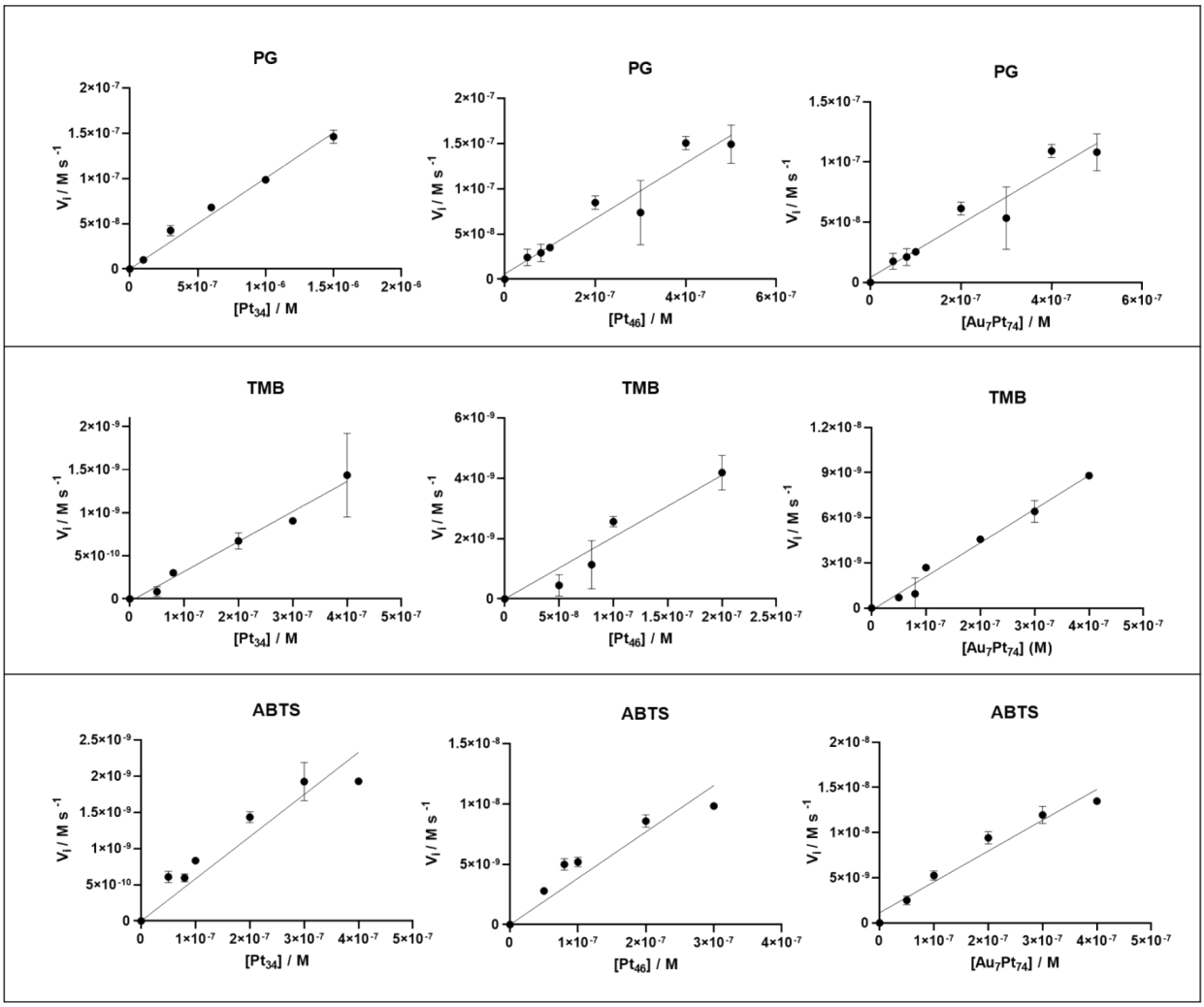

Figure S9. Calculation of the apparent turnover number $^{app}k_{cat}$ for A) PG, B) TMB, and C) ABTS for the nanozymes Pt_{34}, Pt_{46}, and Au_7Pt_{74}, and stabilized by the $C6_{His}$ protein.

6.1.3. Catalase-like activity

The disproportion reaction of the hydrogen peroxide (H_2O_2) was measured using a colorimetric enzyme assay with horseradish peroxidase (HRP) and 2,2′-azino-bis(3-ethylbenzothiazoline-6-sulfonic acid) diammonium salt (ABTS). The activity of the nanozymes is measured in an indirect reaction in which non-consumed H_2O_2 is revealed. In presence of H_2O_2, HRP enzyme can oxidize efficiently ABTS, which product can be monitored at 420 nm.

Nanozymes (final concentration of 1 μM) were incubated with various concentrations of H_2O_2 (ranging from 10 μM to 100 μM) in 50 mM phosphate buffer (PB) at pH 7. The incubation was conducted at room temperature for 20 minutes. The concentration of H_2O_2 was optimized to 50 μM to avoid the generation of a high number of bubbles that could interfere with the measurement. After the incubation, to prevent interference of the nanozymes with ABTS, the catalyst was removed from the reaction using an Amicon 10 kDa cut-off filter. Then, the revealing mixture (sodium phosphate buffer pH 7.0 containing 0.25 mM of ABTS and 10 nM of HRP) was added, and the UV-Vis spectra and the absorbance at 420 nm were measured using a microplate reader. Same procedure was followed to determine the pH profile of the catalase-like activity of the nanozymes. pH higher than 8 could not be measured due to the low activity of HRP enzyme under these conditions.

All the samples were tested in triplicates using the same protocol at pH 7.0 and the UV/Vis spectra monitored. To calculate the efficiency of the disproportion reaction, each of the absorbance values obtained were referred to corresponding control samples to which the nanozymes were not added.

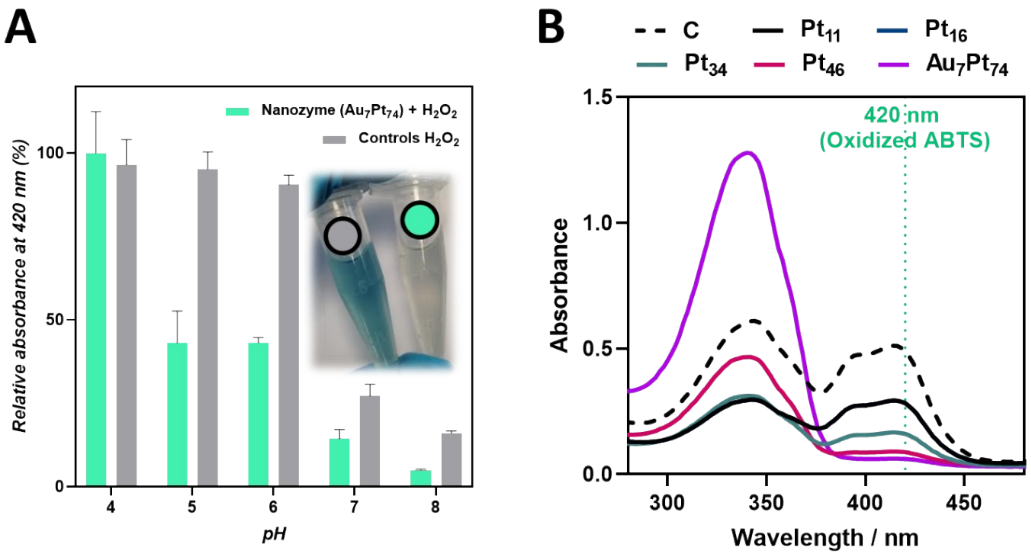

Figure S10. A) Relative absorbance measured at 420 nm after adding 10 nM of HRP and 0.25 mM of ABTS at different pH (from 4 up to 8). The decrease of the signal from control samples at pH 7 and pH 8 can be explained by the lower activity of HRP under these pH values; B) UV-Vis spectra after 50 µM hydrogen peroxide incubation with the variety of Pt-based nanozymes. No peak at 420 nm was observed for the most active nanozymes (Au_7Pt_{74} and Pt_7) confirming the full degradation of hydrogen peroxide after 20 minutes incubation.

6.2. Reduction capability of the nanozymes

6.2.1. Reduction of p-nitrophenols

In a typical reduction experiment, p-nitrophenol (PNP), and $NaBH_4$ were mixed in phosphate buffer (50 mM) pH 8.5 with a final concentration of 0.22 mM (PNP) and 22 mM ($NaBH_4$), respectively, to form bright yellow 4-nitrophenolate ions. After 30 s, nanozymes (1 µM) were added into the PNP+$NaBH_4$ solution and the final reaction volume was kept to 200 µL. Spectral data were collected within the wavelength range of 250 nm to 600 nm, using a step size of 1 nm in microplate reader. Time-dependent kinetic experiments were also conducted by continuously monitoring the absorbance at λ_{max} (400 nm) over a specific duration. Unless otherwise specified, all catalysis experiments were conducted under ambient conditions. Figure S11A illustrates the progress of PNP reduction with time in presence of different nanozymes and Figure S11B shows time dependent kinetic experiments after adding different concentration of most active nanozymes Pt_{46}.

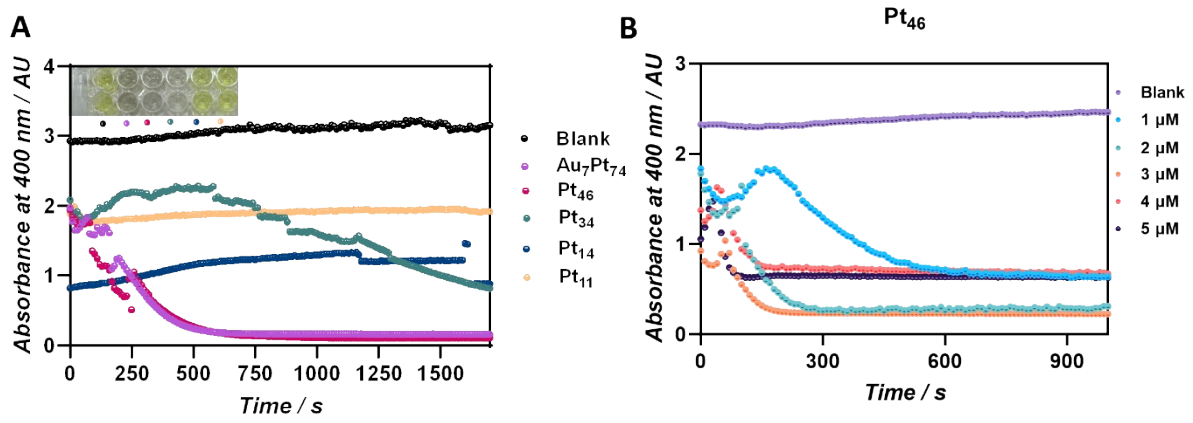

Figure S11. A) Progress of PNP reduction monitored at 400 nm in presence of different nanozymes with varying number of platinum atoms in clusters. B) Gradual decrease in 4-nitrophenolate absorption peak with varying concentration of Pt_{46} nanozyme.

Figure S12 illustrates time dependent absorption spectra of PNP+$NaBH_4$ solution after addition of five different nanozymes, clearly demonstrating the disappearance of 4-nitrophenolate peak at λ_{max} (400 nm) and the appearance of a new peak that corresponds to PAP at λ_{max} (300 nm). For the reduction of PNP, we have monitored the progress of the reaction by measuring the absorbance at 400 nm, where the contribution of the protein absorption at 280 nm for 1 µM concentration was negligible.

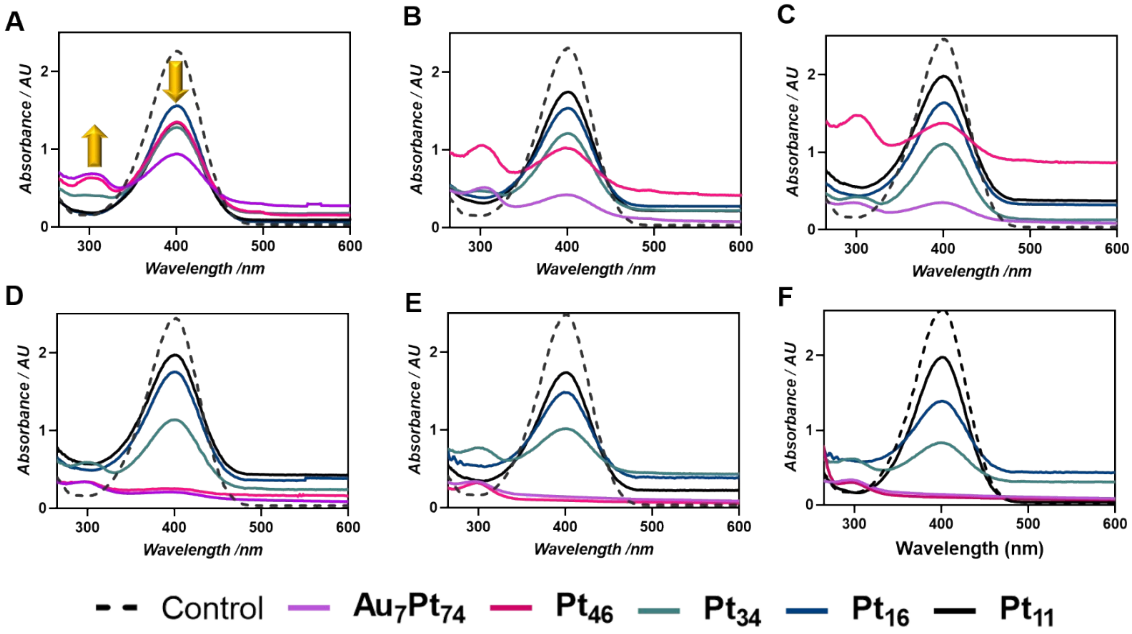

Figure S12. Nanozyme catalyzed PNP reduction. Complete dampening of PNP absorption peak at ~400 nm was observed after 10 minutes in presence of Au_7Pt_{74} and Pt_{46} Absorption spectra at time A) 0, B) 2, C) 5, D) 10, E) 20, and F) 30 minutes, respectively.

6.2.2. Nanozymes in chemoenzymatic sequential reaction to synthesize 4-aminophenol from 4-nitrophenyl butyrate

The hydrolysis of 4-nitrophenol butyrate was performed using CALB enzyme. The enzymatic assay was performed by measuring the increase in absorbance at 400 nm using 0.2 mM of PNB and varying concentrations of CALB (15, 30, 45, and 60 μM) due to release of 4-nitrophenolate ions. After complete conversion of PNB, 1 μM of Au_7Pt_{50} bimetallic hybrid was subsequently added to each solution. Time-dependent kinetic experiments were conducted by continuously monitoring the absorbance at λ_{max} (400 nm) as reported in previous section. Absorption spectra was recorded after completion of reaction demonstrating successful sequential cascade reaction converting PNP to PAP. One pot reaction was also employed by simultaneously adding CALB, PNB, nanozyme (Au_7Pt_{50} -1 μM) in the presence and absence of $NaBH_4$. Figure S13 illustrates increase of the absorption of PNP peak after addition of $NaBH_4$.

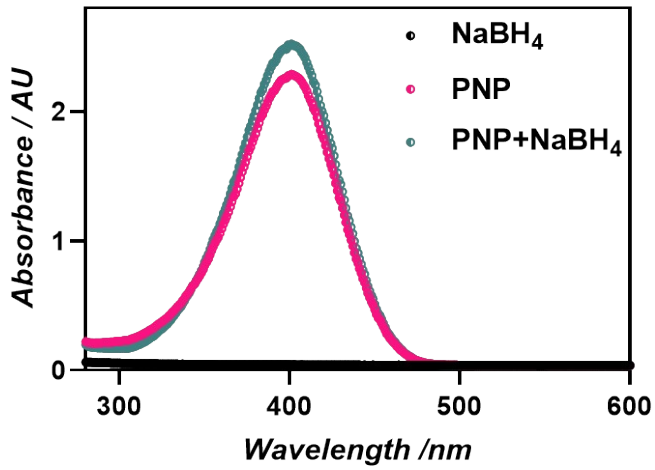

Figure S13. Increase of the absorption at 400 nm of the PNP upon the addition of $NaBH_4$.

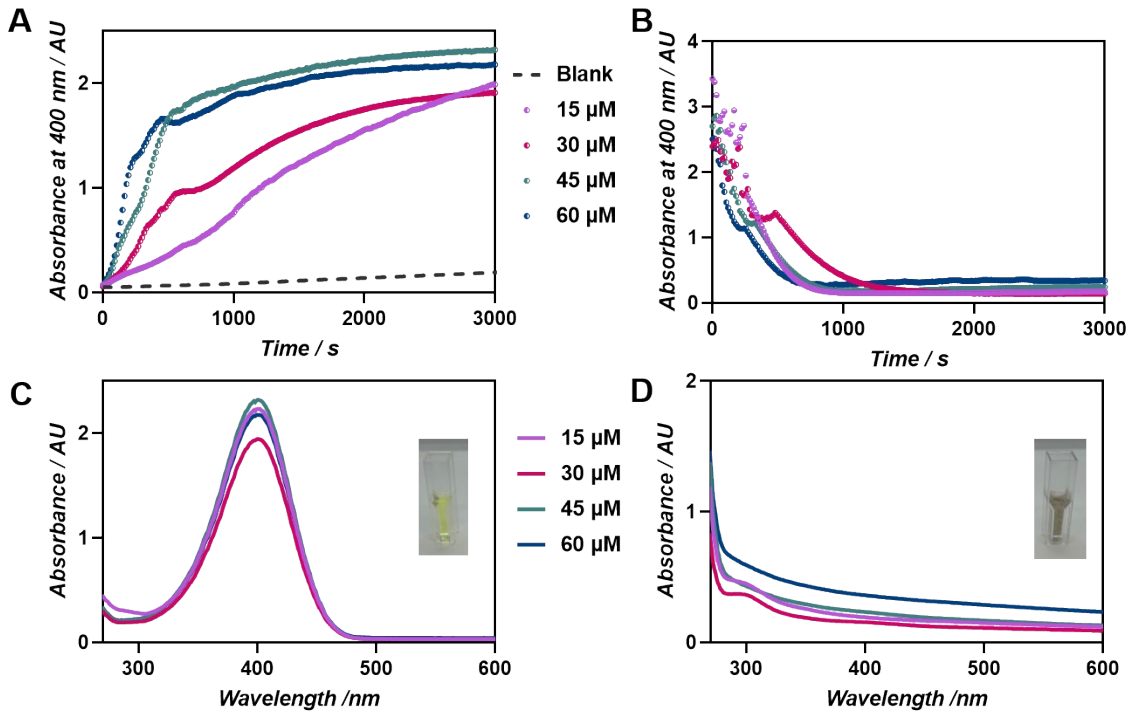

Figure S14. A) Progress of PNB conversion monitored at 400 nm in presence of different concentrations of CALB. B) Gradual decrease in 4-nitrophenolate absorption peak after sequentially adding the nanozyme (Au_7Pt_{50} -1 µM). C) Absorption spectra of the solution after conversion of PNB in presence of CALB (yellow color indicates formation of 4-nitrophenolate). D) Absorption spectra after full conversion to PAP after sequentially adding nanozyme (Au_7Pt_{50} -1 µM) (disappearance of yellow color).

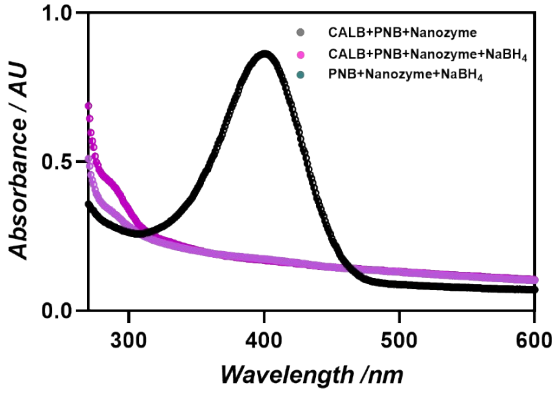

Figure S15. Absorption spectra after 60 minutes of one pot conversion of PNB to PAP by the co-addition of CALB and the nanozyme (Au_7Pt_{50} -1 µM) in presence and absence of $NaBH_4$.

7. References

1. L. Signor, E. B. Erba, *J. Vis. Exp.,* 2013, **79**, e50635.

2. R. L. Domene, S. V. Díaz, E. Modin, A. Beloqui and A. L. Cortajarena, *Adv. Funct. Mater.* 2023, 2301131.

3. A. Aires, I. Llarena, M. Moller, J. C. Smirnov, J. C. Gonzalez, A. L. Cortajarena, *Angew. Chem.,* 2019, **58**, 6214–6219.